Cooperative Sensing in Automotive Urban Scenarios Using Poisson Line Processes

François De Saint Moulin*, Charles Wiame†, Claude Oestges‡, Luc Vandendorpe§
ICTEAM, UCLouvain - Louvain-la-Neuve, Belgium
*francois.desaintmoulin †charles.wiame ‡claude.oestges §luc.vandendorpe@uclouvain.be

***Abstract*—In this paper, we consider a cooperative sensing model for automotive urban scenarios studied within a stochastic geometry framework. The street deployment is modelled by means of a Poisson line process and the active roadside units within each street via homogeneous Poisson point processes. The RSUs located in proximity of the typical vehicle cooperate in order to detect it in crossroad and non-crossroad situations, improving the overall sensing performance. Multiple cooperation schemes are analysed. The model is validated thanks to Monte-Carlo simulations.**

***Index Terms*—stochastic geometry, Poisson line process, automotive scenario, radar, CoMP**

I. Introduction

Sensing systems are a key technology for today and future vehicles and smart cities, helping with tasks such as parking, cruise control and the development of autonomous vehicles. In smart cities, the detection of vehicles and the cooperation between the user equipments and the infrastructure is crucial to improve the safety of autonomous vehicles at crossroads. To enhance the reliability of such technologies, cooperative sensing is a promising solution in urban automotive scenarios. The evaluation of the sensing performance achieved with and without cooperation in such situations is therefore required.

In order to assess the performance of the network at a large scale level, stochastic geometry has been used in this work. It enables to obtain closed-form expressions for performance metrics by averaging over realisations of random point processes modelling the network nodes positions [1]. For radar applications in automotive scenarios, [2] evaluates the performance achieved for different radar cross section models. Multiple lanes are considered in [3] and [4], the former considering front- and side-mounted radars with directional antenna patterns, and the latter taking into account the interference from reflections on vehicles in the neighbouring lanes. In these papers, Poisson Point Processes (PPP) are usually chosen to model the nodes positions. Instead, [5] uses a one-dimensional lattice, and [6], [7] use Matérn hard-core processes, respectively in one or two dimensions. Fine-grained analysis is applied in [8], [9] to evaluate the meta distribution of the Signal to Interference plus Noise Ratio (SINR), enabling to analyse the reliability of the detection at each individual vehicle. Recently, joint radar and communication applications have also been analysed. For automotive applications, [10] and [11] evaluate the cooperative detection range of the system, respectively with spectrum allocation between both functions or with joint systems.

François De Saint Moulin is a Research Fellow of the Fonds de la Recherche Scientifique - FNRS.

In order to enhance the large-scale modelling of cities, Poisson line processes have been recently introduced for communication networks [12]–[14]. Additionally, to further improve the network performance, Cooperative MultiPoint (CoMP) joint transmission schemes have been introduced [15], [16]. More specifically, for cooperative sensing, [17] evaluates the sensing capabilities in a joint radar communication scenario with three different cooperation rules, namely the OR, Majority (MAJ) and AND rule. The spatial distribution of the base stations follows a β-Ginibre point process to model the repulsion behaviour.

To our best knowledge, the sensing performance obtained with CoMP schemes in large-scale cities modelled with Poisson line processes have not yet been evaluated. Based on the aforementioned works, the contributions of this paper are summarised as follows:

- An automotive urban scenario is modelled using a poisson line process. Multiple road side units cooperate to detect successfully the typical node. The achieved performance is obtained using stochastic geometry in crossroads with an arbitrary number of roads, and validated through Monte-Carlo (MC) simulations.
- Leveraging on [17], multiple cooperation schemes are analysed for the cooperative sensing: the K rule (OR rule if $K = 1$), the MAJ rule and the AND rule.
- Numerous interference sources are considered for each cooperative RoadSide Unit (RSU), namely direct links, reflections on the typical node and diffractions.

II. System Model

A. Considered scenario

In the considered city, all the roads are modelled following a Poisson Line Process (PLP) $\mathbf{\Xi}_{\mathrm{R}}$ composed of multiple lines $L_i \in \mathbb{R}^2$. These lines are characterised by their perpendicular distances $y_i \in [0, \infty[$ to the origin, and their angles $\theta_i \in [0, 2\pi[$, as illustrated in [12]. The line L_0 is an horizontal line crossing the origin, i.e. $y_0 = 0$ and $\theta_0 = \frac{\pi}{2}$.

The typical vehicle is located at the origin of the line L_0. Since the performance at the typical vehicle is strongly impacted by its location on the street, the overall metric can be computed as a weighted average, depending on the

probability to be located in an intersection with $N_{\mathrm{R}}+1$ lanes. If $N_{\mathrm{R}}=0$, there is no intersection. If $N_{\mathrm{R}}>0$ instead, the lines $L_1,...,L_{N_{\mathrm{R}}}$ are crossing the origin, i.e. $y_i=0\,\forall\, i=1,...,N_{\mathrm{R}}$. The other perpendicular distances are distributed following a 1D PPP $\mathbf{\Phi}_{\mathrm{y}}=\{y_{N_{\mathrm{R}}+1},y_{N_{\mathrm{R}}+2},...\}\in\mathbb{R}^{+}$ of density λ_{y}. RSUs are then modelled on every line L_i following a 1D PPP $\mathbf{\Phi}_{\mathrm{v}i}$ of density $\lambda_{\mathrm{r}i}$. We assume that they are equipped with omnidirectional antennas. The angles of all the lines except L_0 are distributed following a Cox line process, meaning that they are distributed uniformly in $[0,2\pi[$. The Manhattan process is obtained as a particular case of the Cox line process. We consider that all RSUs at a distance lower than ρ in the lines $\{L_0,...,L_{N_{\mathrm{R}}}\}$ are cooperating. The set of cooperating nodes in road i is denoted $\mathcal{C}_i$.

B. Propagation models

With a linear path-loss model, the typical vehicle being positioned at position $(0,0)$, we assume that the received power at a node located at position $\mathbf{z}_1$ from a transmitter located at position $\mathbf{z}_2$, potentially located in two different roads forming an angle ψ with an intersection at position $\boldsymbol{\chi}$, can be written as

$$P=\kappa\, g(\mathbf{z}_1,\mathbf{z}_2,\boldsymbol{\chi},\psi)^{-\alpha}\,\gamma, \tag{1}$$

where γ is an exponentially distributed random variable modelling the small-scale fading of the link. The parameters κ, α and the function g are set depending on the considered link. For the useful radar echo, the transmitter is also the receiver, and $g(\mathbf{z}_1)=2\|\mathbf{z}_1\|$. For the interference, three different interference types are considered (Figure 1):

1) The interference generated by direct links between different RSUs on the same road, so-called *interference of type I* in this paper, for which $g(\mathbf{z}_1,\mathbf{z}_2)=\|\mathbf{z}_1-\mathbf{z}_2\|$.
2) The interference generated by reflection on the typical node, so-called *interference of type II* in this paper, for which $g(\mathbf{z}_1,\mathbf{z}_2,\psi)=\left(\frac{1+\cos\psi}{2}\right)^{-\frac{\nu_r}{\alpha}}(\|\mathbf{z}_1\|+\|\mathbf{z}_2\|)$, as proposed in [18]. The parameter ν_r defines the angular beamwidth of the reflective contribution.
3) The interference generated by diffraction, so-called *interference of type III* in this paper, for which the Berg model [19] proposes $g(\mathbf{z}_1,\mathbf{z}_2,\boldsymbol{\chi},\psi)=\|\mathbf{z}_1-\boldsymbol{\chi}\|+\|\mathbf{z}_2-\boldsymbol{\chi}\|+k_b\left(\frac{2\psi}{\pi}\right)^{\nu_b}\|\mathbf{z}_1-\boldsymbol{\chi}\|\|\mathbf{z}_2-\boldsymbol{\chi}\|$, where $k_b=\sqrt{q_b f_c/c}$, and ν_b and q_b are empirical parameters.

III. Mathematical Development

Let us denote respectively by R_{ji}, $I_{\mathrm{R}ji}$ and W_{ji} the power of the radar echo, the total interference and the noise at the cooperative RSU i located at position x_{ji} in the lane L_j of the crossroad. This RSU performs a successful detection if the SINR $R_{ji}/(I_{\mathrm{R}ji}+W_{ji})$ is higher than a given SINR threshold η_{R}. Therefore, its success probability is defined as

$$\mathcal{P}_{\mathrm{S}ji}(\eta_{\mathrm{R}})=\mathbb{P}\left(\frac{R_{ji}}{I_{\mathrm{R}ji}+W_{ji}}\geq\eta_{\mathrm{R}}\right). \tag{2}$$

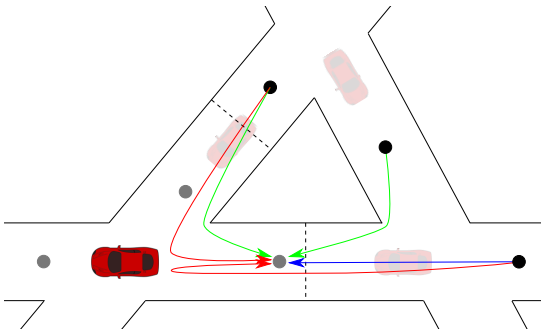

Fig. 1. Different interference types affecting the cooperative RSUs. The interference generated by direct links, reflection on the typical node and diffraction are respectively drawn in blue, red and green. Note that the same interference types occurs between different cooperative RSUs. The lanes are linear with the PLP model and the lanes width is only illustrated for clarity.

Following the propagation models presented in Section II-B, the radar echo power R_{ji} is expressed as

$$R_{ji}=\kappa_{\mathrm{R}}\,|x_{ji}|^{-\alpha}\,\gamma_{ji}. \tag{3}$$

The total interference aggregates multiple interference sources:

1) The interference of type I and II from the RSUs in the road j which are not cooperating:

$$I_{\mathrm{R}1ji}=\sum_{k|z_{jk}\in\mathbf{\Phi}_{\mathrm{v}j}\setminus\mathcal{C}_j}\Big(\kappa_{\mathrm{I}}|x_{ji}-z_{jk}|^{-\alpha}\,\gamma^{(\mathrm{I})}_{1,jik} + \kappa_{\mathrm{I}}\left(|x_{ji}|+|z_{jk}|\right)^{-\alpha}\mathbb{1}\left(x_{ji}z_{jk}>0\right)\,\gamma^{(\mathrm{II})}_{1,jik}\Big). \tag{4}$$

The interference of type II only occurs when the cooperative and interfering RSUs are on the same side of the typical node.

2) The interference of type I and II from the RSUs in the road j which are cooperating:

$$I_{\mathrm{R}2ji}=\sum_{k|x_{jk}\in\mathcal{C}_j\setminus\{x_{ji}\}}\Big(\kappa_{\mathrm{I}}|x_{ji}-x_{jk}|^{-\alpha}\,\gamma^{(\mathrm{I})}_{2,jik} + \kappa_{\mathrm{I}}\left(|x_{ji}|+|x_{jk}|\right)^{-\alpha}\mathbb{1}\left(x_{ji}x_{jk}>0\right)\,\gamma^{(\mathrm{II})}_{2,jik}\Big). \tag{5}$$

If some mitigation mechanism is introduced between the cooperative RSUs, this term can be reduced or deleted.

3) The interference of type II and III from the RSUs in the road $l\neq j$ belonging to the crossroad which are not cooperating:

$$I_{\mathrm{R}3ji}=\sum_{l\neq j}^{N_{\mathrm{R}}}\sum_{k|z_{lk}\in\mathbf{\Phi}_{\mathrm{v}l}\setminus\mathcal{C}_j}\Big(\kappa_{\mathrm{I}}\,\mu(\theta_j,\theta_l)\,\left(|x_{ji}|+|z_{lk}|\right)^{-\alpha} \gamma^{(\mathrm{II})}_{3,jilk}+\kappa_{\mathrm{I}}\,B_1(x_{ji},z_{lk},\theta_j,\theta_l)^{-\alpha}\,\gamma^{(\mathrm{III})}_{3,jilk}\Big), \tag{6}$$

with

$$\mu(\theta_j,\theta_l)=\left(\frac{1+\cos(\psi_{jl}(\theta_j,\theta_l))}{2}\right)^{\nu_r}, \tag{7}$$

$$B_1(x_{ji},z_{lk},\theta_j,\theta_l)= |x_{ji}|+|z_{lk}|+\left(\frac{2\psi_{jl}(\theta_j,\theta_l))}{\pi}\right)^{\nu_b}|x_{ji}||z_{lk}|, \tag{8}$$

and ψ_{jl} being the angle between the roads j and l:

$$\psi_{jl}(\theta_j,\theta_l)=\left|\theta_j-\pi\left\lfloor\frac{\theta_j}{\pi}+\frac{1}{2}\right\rfloor\right|+\left|\theta_l-\pi\left\lfloor\frac{\theta_l}{\pi}+\frac{1}{2}\right\rfloor\right|. \tag{9}$$

4) The interference of type II and III from RSUs in the road $l\neq j$ belonging to the crossroad which are cooperating:

$$I_{\mathrm{R}4ji}=\sum_{l\neq j}^{N_\mathrm{R}}\sum_{k|x_{lk}\in\mathcal{C}_j}\Big(\kappa_\mathrm{I}\,\mu(\theta_j,\theta_l)\;(|x_{ji}|+|x_{lk}|)^{-\alpha}\;\gamma_{4,jilk}^{(\mathrm{II})}+\kappa_\mathrm{I}\,B_1(x_{ji},x_{lk},\theta_j,\theta_l)^{-\alpha}\,\gamma_{4,jilk}^{(\mathrm{III})}\Big), \tag{10}$$

with the functions μ and B_1 defined above. Again, if some mitigation mechanism is introduced between the cooperative RSUs, this can be reduced or deleted.

5) The interference of type III from i RSUs in the road $l\neq j$ not belonging to the crossroad:

$$I_{\mathrm{R}5ji}=\sum_{l=N_\mathrm{R}+1}^{\infty}\sum_{k|z_{lk}\in\mathbf{\Phi}_{\mathrm{v}l}}\kappa_\mathrm{I}\,B_2(x_{ji},z_{lk},\theta_j,\theta_l,y_l)^{-\alpha}\,\gamma_{5,jilk}^{(\mathrm{III})}, \tag{11}$$

with the function B_2 being the Berg distance defined in Section II-B. The vectors $\mathbf{z}_1-\boldsymbol{\chi}$ and $\mathbf{z}_2-\boldsymbol{\chi}$ are computed using the absolute positions of the two RSUs and the absolute position of the intersection between the two lanes. The angle between the two lanes is computed based on the scalar product between these vectors.

In this paper, we consider the success probability achieved by combining the decisions made by the cooperative RSUs. At the central unit, the decisions are gathered to determine if a target is detected successfully or not depending on the adopted cooperation scheme: the K rule (equivalent to the OR rule when $K=1$), MAJ rule or AND rule. In the following, let us denote by n_j the number of cooperative RSUs in lane j of the crossroad, and $[\mathbf{n}]_j=n_j$. We will assume that this number is known for each lane in the crossroad. The total number of cooperative RSUs $n_T=n_0+...+n_{N_\mathrm{R}}$ is therefore also known. In that case, the MAJ rule and AND rule are respectively obtained by setting $K=\left\lceil\frac{n_T}{2}\right\rceil$ and $K=n_T$. Otherwise, the metric can be averaged: as the RSUs are distributed following independent homogeneous PPPs on the lanes, the joint probability density function of the numbers of cooperative RSUs on each lane in the crossroad is given by

$$f_{\mathbf{n}}(\mathbf{n})=\frac{(2\lambda_\mathrm{r}\rho)^{n_T}}{n_0!\dots n_{N_\mathrm{R}}!}\exp\left(-2(N_\mathrm{R}+1)\lambda_\mathrm{r}\rho\right)\;\mathbb{1}\left(\mathbf{n}\in\mathbb{N}^{N_\mathrm{R}+1}\right), \tag{12}$$

and the cooperative success probability is computed as $\mathcal{P}_\mathrm{S}{}^{(K)}(\eta_\mathrm{R})=\sum_{\mathbf{n}}f_{\mathbf{n}}(\mathbf{n})\,\mathcal{P}_\mathrm{S}{}^{(K)}(\eta_\mathrm{R}|\mathbf{n})$. In that case, the MAJ rule and AND rule are not equivalent to the K rule since with the K rule, K is constant whatever the total number of cooperative RSUs. However, they are computed using the K rule by modifying K depending on the total number of cooperative RSUs.

With the K rule, the detection is successful if at least K RSUs agree on the presence of a target. As in [17], the cooperative success probability conditioned on the number of cooperative RSUs is expressed as

$$\mathcal{P}_\mathrm{S}{}^{(K)}(\eta_\mathrm{R}|\mathbf{n})=\mathbb{E}_{-\backslash\boldsymbol{\gamma}}\left[\sum_{k=K}^{n_T}\sum_{m=1}^{\binom{n_T}{k}}\prod_{j=0}^{N_\mathrm{R}}\prod_{i=1}^{n_j}\mathcal{P}_{\mathrm{S}ji}^{\,\delta_{ji}^{(m)}}(\eta_\mathrm{R})\left(1-\mathcal{P}_{\mathrm{S}ji}(\eta_\mathrm{R})\right)^{1-\delta_{ji}^{(m)}}\right], \tag{13}$$

where $\mathbb{E}_{-\backslash\boldsymbol{\gamma}}$ denotes the expectation over every random quantity, except the small-scale fading coefficients of all the useful radar echoes $\boldsymbol{\gamma}=\{\gamma_{ji}\}_{\substack{j=0,\dots,N_\mathrm{R}\\ i=0,\dots,n_j-1}}$, assumed to be independent with each other. It takes into account every combination of K or more than K RSUs detecting a target in the cooperative set. The binary value $\delta_{ji}^{(m)}$ defines if the cooperative RSU i in the road j of the crossroad successfully performs or not a detection for each considered combination m. In order to simplify this expression, we have developed Lemma 1.

Lemma 1: *The polynomial of* (13) *can be developed as*

$$\sum_{k=K}^{n_T}\sum_{m=1}^{\binom{n_T}{k}}\prod_{j=0}^{N_R}\prod_{i=1}^{n_j}\mathcal{P}_{Sji}^{\,\delta_{ji}^{(m)}}(\eta_R)\left(1-\mathcal{P}_{Sji}(\eta_R)\right)^{1-\delta_{ji}^{(m)}}=\sum_{m=1}^{2^{n_T}-1}a^{(m)}\prod_{j=0}^{N_R}\prod_{i=1}^{n_j}\mathcal{P}_{Sji}^{\,b_{ji}^{(m)}}(\eta_R). \tag{14}$$

In this expression, $b_{ji}^{(m)}$ is a binary value which varies for each term of the summation over the $2^{n_T}-1$ binary words $\mathbf{b}^{(m)}=\{b_{ij}^{(m)}\}_{\substack{j=0,\dots,N_\mathrm{R}\\ i=0,\dots,n_j-1}}$ of size n_T which are non zero. If the cardinality of $\mathbf{b}^{(m)}$ is denoted by $\|\mathbf{b}^{(m)}\|_1=c^{(m)}$, the coefficient $a^{(m)}$ is computed as

$$a^{(m)}=\begin{cases}(-1)^{c^{(m)}-K}\,\dfrac{c^{(m)}-K+1}{c^{(m)}}\binom{c^{(m)}}{K-1} & \text{if } c^{(m)}\geq K,\\ 0 & \text{otherwise.}\end{cases}$$

Proof: This result is obtained by developing the product of (14) and summing/subtracting the number of time each product between the success probabilities of the cooperative RSUs appears. Every product containing the same number of elements (related to the cardinality of $\mathbf{b}^{(m)}$ defined as $c^{(m)}$) is associated with the same coefficient given by $\sum_{p=0}^{c^{(m)}-k}(-1)^p\binom{c^{(m)}}{c_m-p}$, which leads to (1). ■

Hence, the cooperative success probability conditioned on the number of cooperative nodes is expressed as

$$\mathcal{P}_\mathrm{S}{}^{(K)}(\eta_\mathrm{R}|\mathbf{n})=\sum_{m=1}^{2^{n_T}-1}a^{(m)}\mathbb{E}_{-\backslash\boldsymbol{\gamma}}\left[\prod_{j=0}^{N_\mathrm{R}}\prod_{i=1}^{n_j}\mathcal{P}_{\mathrm{S}ji}^{\,b_{ji}^{(m)}}(\eta_\mathrm{R})\right]. \tag{15}$$

Let us denote by $\mathbf{x}=\{x_{ji}\}_{\substack{j=0,\dots,N_\mathrm{R}\\ i=0,\dots,n_j-1}}$ the positions of the cooperative RSUs and $\boldsymbol{\theta}=\{\theta_j\}_{j=0,\dots,N_\mathrm{R}}$ the angles of the lanes in the crossroad. Proposition 1 provides the expression of the expectation in (15).

$$g_{13}^{(m)}(\mathbf{x},\boldsymbol{\theta}) = \prod_{j=0}^{N_\mathrm{R}} \exp\Bigg(-\lambda_\mathrm{r} \int_{-\infty}^{\infty} \Bigg(1 - \prod_{i=0}^{n_j-1} \frac{1}{1+\frac{b_{ji}^{(m)}\eta_\mathrm{R}\kappa_\mathrm{I}|x_{ji}-z|^{-\alpha}}{\kappa_\mathrm{R}|x_{ji}|^{-\alpha}}} \cdot \frac{1}{1+\frac{b_{ji}^{(m)}\eta_\mathrm{R}\kappa_\mathrm{I}(|x_{ji}|+|z|)^{-\alpha}\mathbb{1}(x_{ji}z>0)}{\kappa_\mathrm{R}|x_{ji}|^{-\alpha}}} \prod_{l\neq j}^{N_\mathrm{R}} \prod_{i=0}^{n_l-1} \frac{1}{1+\frac{b_{li}^{(m)}\eta_\mathrm{R}\kappa_\mathrm{I}\mu(\theta_j,\theta_l)(|x_{li}|+|z|)^{-\alpha}}{\kappa_\mathrm{R}|x_{li}|^{-\alpha}}} \cdot \frac{1}{1+\frac{b_{li}^{(m)}\eta_\mathrm{R}\kappa_\mathrm{I}B_1(x_{li},z,\theta_j,\theta_l)^{-\alpha}}{\kappa_\mathrm{R}|x_{li}|^{-\alpha}}} \Bigg)\mathrm{d}z \Bigg), \tag{16}$$

$$g_{2}^{(m)}(\mathbf{x}) = \prod_{j=0}^{N_\mathrm{R}} \prod_{i=0}^{n_j-1} \prod_{k|x_{jk}\in\mathcal{C}_j\setminus\{x_{ji}\}} \frac{1}{1+\frac{b_{ji}^{(m)}\eta_\mathrm{R}\kappa_\mathrm{I}|x_{ji}-x_{jk}|^{-\alpha}}{\kappa_\mathrm{R}|x_{ji}|^{-\alpha}}} \cdot \frac{1}{1+\frac{b_{ji}^{(m)}\eta_\mathrm{R}\kappa_\mathrm{I}(|x_{ji}|+|x_{jk}|)^{-\alpha}\mathbb{1}(x_{ji}x_{jk}>0)}{\kappa_\mathrm{R}|x_{ji}|^{-\alpha}}}, \tag{17}$$

$$g_{4}^{(m)}(\mathbf{x},\boldsymbol{\theta}) = \prod_{j=0}^{N_\mathrm{R}} \prod_{i=0}^{n_j-1} \prod_{l\neq j}^{N_\mathrm{R}} \prod_{k|x_{lk}\in\mathcal{C}_l} \frac{1}{1+\frac{b_{ji}^{(m)}\eta_\mathrm{R}\kappa_\mathrm{I}\mu(\theta_j,\theta_l)(|x_{ji}|+|x_{lk}|)^{-\alpha}}{\kappa_\mathrm{R}|x_{ji}|^{-\alpha}}} \cdot \frac{1}{1+\frac{b_{ji}^{(m)}\eta_\mathrm{R}\kappa_\mathrm{I}B_1(x_{ji},x_{lk},\theta_j,\theta_l)^{-\alpha}}{\kappa_\mathrm{R}|x_{ji}|^{-\alpha}}}, \tag{18}$$

$$g_{5}^{(m)}(\mathbf{x},\boldsymbol{\theta}) = \exp\Bigg(-\lambda_\mathrm{y} \int_0^{\infty} \Bigg(1 - \frac{1}{2\pi}\int_0^{2\pi} \exp\Bigg(-\lambda_\mathrm{r}\int_{-\infty}^{\infty} \Bigg(1 - \prod_{j=0}^{N_\mathrm{R}}\prod_{i=0}^{n_j-1} \frac{1}{1+\frac{b_{ji}^{(m)}\eta_\mathrm{R}\kappa_\mathrm{I}B_2(x_{ji},z,\theta_j,\theta,y)^{-\alpha}}{\kappa_\mathrm{R}|x_{ji}|^{-\alpha}}} \Bigg)\mathrm{d}z \Bigg)\mathrm{d}\theta \Bigg)\mathrm{d}y \Bigg), \tag{19}$$

$$g_{W}^{(m)}(\mathbf{x}) = \prod_{j=0}^{N_\mathrm{R}} \prod_{i=0}^{n_j-1} \exp\left(-\frac{b_{ji}^{(m)}\eta_\mathrm{R} W}{\kappa_\mathrm{R}|x_{ji}|^{-\alpha}} \right) \tag{20}$$

$$\mathcal{P}_\mathrm{S}{}^{(K)}(\eta_\mathrm{R}|\mathbf{n},\mathbf{x},\boldsymbol{\theta}) = \sum_{m=1}^{2^{n_T}-1} a^{(m)}\, g_{13}^{(m)}(\mathbf{x},\boldsymbol{\theta})\, g_{2}^{(m)}(\mathbf{x})\, g_{4}^{(m)}(\mathbf{x},\boldsymbol{\theta})\, g_{5}^{(m)}(\mathbf{x},\boldsymbol{\theta})\, g_{W}^{(m)}(\mathbf{x}). \tag{21}$$

Proposition 1: *Assuming that the positions* $\mathbf{x}$ *of the cooperative RSUs and the angles* $\boldsymbol{\theta}$ *of the lanes in the crossroad are known, the expectation of* (15) *is developed as*

$$\mathbb{E}_{-\setminus\gamma}\left[\prod_{j=0}^{N_\mathrm{R}}\prod_{i=1}^{n_j} \mathcal{P}_{\mathrm{S}ji}^{\,b_{ji}^{(m)}}(\eta_\mathrm{R}) \,\middle|\, \mathbf{x},\boldsymbol{\theta} \right] = g_{13}^{(m)}(\mathbf{x},\boldsymbol{\theta})\, g_{2}^{(m)}(\mathbf{x})\, g_{4}^{(m)}(\mathbf{x},\boldsymbol{\theta})\, g_{5}^{(m)}(\mathbf{x},\boldsymbol{\theta})\, g_{W}^{(m)}(\mathbf{x}), \tag{22}$$

where the g functions are defined in (16)-(20)*.*

Proof: Knowing that the small-scale fading coefficients are independent and exponentially distributed, the expectation of (15) is developed as

$$\mathbb{E}\left[\prod_{j=0}^{N_\mathrm{R}}\prod_{i=1}^{n_j} \exp\left(-\frac{b_{ji}^{(m)}\eta_\mathrm{R} I_{\mathrm{R}ji}}{\kappa_\mathrm{R}\,|x_{ji}|^{-\alpha}} \right) \exp\left(-\frac{b_{ji}^{(m)}\eta_\mathrm{R} W_{ji}}{\kappa_\mathrm{R}\,|x_{ji}|^{-\alpha}} \right) \right].$$

The aggregate interference $I_{\mathrm{R}ji}$ can be split following the five interference sources detailed in this section. In order to simplify the expression, the expectations over the small-scale fading coefficients are first applied separately on each term since they are independent. Then, the Probability Generating FunctionaLs (PGFL) over $\boldsymbol{\Phi}_{\mathrm{v}0}, ..., \boldsymbol{\Phi}_{\mathrm{v}N_\mathrm{R}}$ are applied on $I_{\mathrm{R}1}$ and $I_{\mathrm{R}3}$ with the product on i inside the PGFL. Finally, for $I_{\mathrm{R}5}$, a PGFL over $\boldsymbol{\Phi}_\mathrm{y}$ is first applied, then an expectation about the angle of the lane outside the crossroad, and a PGFL over the vehicles PPP of this lane. ■

The cooperative success probability conditioned on the number of cooperative RSUs is finally computed by averaging (21) over the positions $\mathbf{x}$ of the cooperative RSUs and the angles $\boldsymbol{\theta}$ of the lanes in the crossroad.

TABLE I
SIMULATION PARAMETERS.

Parameter	Value
Roads density	$\lambda_\mathrm{y} = 0.025$ [m^{-1}]
RSUs density	$\lambda_\mathrm{r} = 0.05$ [m^{-1}]
Cooperative distance	$\rho = 50$ [m]
Path-loss parameters	$\kappa_\mathrm{R} = \kappa_\mathrm{I} = 10^{-6}$, $\alpha = 2$
Reflection parameters	$\nu_r = 4$
Diffraction parameters	$k_b = 1.58$ [m^{-1}], $\nu_b = 1.5$
With fixed $\mathbf{n}$, $\mathbf{x}$, $\boldsymbol{\theta}$ (for Figure 2, top)	
Number of lanes	$N_\mathrm{R}+1 = 2$
Lanes angles	$\boldsymbol{\theta} = \{90°, 45°\}$
Coop. RSUs repartition	$\mathbf{n} = \{6, 4\}$ (10 RSUs)
Coop. RSUs positions (1th lane)	$\mathbf{x}_0 = \{-45, -21, -8, 3, 18, 34\}$ [m]
Coop. RSUs positions (2nd lane)	$\mathbf{x}_1 = \{-15, 6, 23, 32\}$ [m]

IV. NUMERICAL ANALYSIS

In this section, the mathematical expressions of the cooperative success probability are first validated with MC simulations through a first scenario in which the number of cooperative RSUs, their positions and the angles of the lanes in the crossroad are known (Dirac delta distribution for these parameters in Figure 2, top). Then, the cooperative success probability is analysed through MC simulations in the general case where all these parameters are unknown (Figure 2, bottom). The characteristic parameters of the distributions are summarised

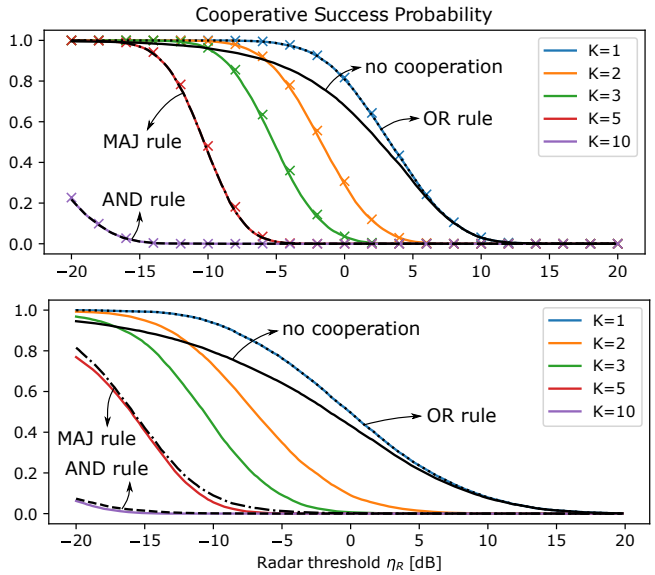

Fig. 2. Success probability with (top) and without (bottom) fixed $\mathbf{n}$, $\mathbf{x}$, $\boldsymbol{\theta}$, achieved by (i) the closest RSU in solid black, (ii) the cooperative RSUs with the K rule in solid colors, (iii) the OR rule in dotted black, (iv) the MAJ rule in dash-dotted black, and (v) the AND rule in dashed black. Crosses denotes the results obtained for the top graph through Monte-Carlo simulations.

in Table I. In the first case where the scenario is fixed, since the number of nodes has been fixed to 10, the AND rule is equivalent to the K rule with $K = 10$, and the MAJ rule is equivalent to the K rule with $K = 5$. This is not the case when the scenario is not fixed anymore. However, the mean number of cooperative RSUs is equal to $2(N_{\mathrm{R}}+1)\rho = 10$, and therefore the performances achieved with the AND and MAJ rules are respectively close to the performances achieved with the K rule, with $K = 10$ and $K = 5$. Compared to the case without any cooperation, in which only the closest RSU detects the target, the OR rule (and the K rule with $K = \{1, 2, 3\}$ for low SINR radar thresholds) enables to achieve a better success probability. However, it is achieved at the price of a higher false alarm probability. By contrast, the MAJ and AND rules achieve lower success probabilities, but the number of false alarms is reduced. The rule should be selected depending on the requirements of the scenario: to achieve a low false alarm probability, the AND rule (or rules with a high K/n_T ratios) should be selected. Contrariwise, the OR rule (or rules with low K/n_T ratios) should be preferred if detections are critical. Nevertheless, for similar false alarm probabilities, the cooperation enables to improve the detection performance.

V. Conclusion

In this paper, we studied the success probability of multiple RSUs cooperating to make a decision using different schemes in an automotive scenario modelled with a PLP. The model was validated through simulations and showed that cooperation helps to improve the sensing performance. However, the cooperation rule should be chosen wisely depending on the requirements in term of detection and false alarm probabilities. Future work includes the optimisation of the RSUs density, the evaluation of other performance metrics, as well as comparisons with measurements or ray-tracing simulations and the extension of the model for integrated sensing and communication systems.

References

[1] Y. Hmamouche, M. Benjillali, S. Saoudi, H. Yanikomeroglu, and M. D. Renzo, "New Trends in Stochastic Geometry for Wireless Networks: A Tutorial and Survey," *Proceedings of the IEEE*, vol. 109, no. 7, pp. 1200–1252, 2021.

[2] Z. Fang, Z. Wei, X. Chen, H. Wu, and Z. Feng, "Stochastic geometry for automotive radar interference with RCS characteristics," *IEEE Wireless Communications Letters*, vol. 9, no. 11, pp. 1817–1820, 2020.

[3] P. Chu, J. A. Zhang, X. Wang, Z. Fei, G. Fang, and D. Wang, "Interference Characterization and Power Optimization for Automotive Radar with Directional Antenna," *IEEE Transactions on Vehicular Technology*, vol. 69, no. 4, pp. 3703–3716, 2020.

[4] Z. Fang, Z. Wei, H. Ma, X. Chen, and Z. Feng, "Analysis of Automotive Radar Interference among Multiple Vehicles," *2020 IEEE Wireless Communications and Networking Conference Workshops, WCNCW 2020 - Proceedings*, 2020.

[5] A. Al-Hourani, R. J. Evans, S. Kandeepan, B. Moran, and H. Eltom, "Stochastic Geometry Methods for Modeling Automotive Radar Interference," *IEEE Transactions on Intelligent Transportation Systems*, vol. 19, no. 2, pp. 333–344, 2018.

[6] L. Kui, S. Huang, and Z. Feng, "Interference analysis for automotive radar using matern hard-core point process," in *2021 IEEE/CIC International Conference on Communications in China (ICCC)*, pp. 817–822, 2021.

[7] K. V. Mishra, B. Shankar M. R., and B. Ottersten, "Stochastic-Geometry-Based Interference Modeling in Automotive Radars Using Matérn Hard-Core Process," *IEEE National Radar Conference - Proceedings*, vol. 2020-Septe, 2020.

[8] G. Ghatak, S. S. Kalamkar, Y. Gupta, and S. Sharma, "A Fine-Grained Analysis of Radar Detection in Vehicular Networks," vol. 9545, no. c, pp. 01–06, 2022.

[9] G. Ghatak, S. Kalamkar, and Y. Gupta, "Radar detection in vehicular networks: Fine-grained analysis and optimal channel access," *IEEE Transactions on Vehicular Technology*, pp. 1–1, 2022.

[10] H. Ma, Z. Wei, X. Chen, Z. Fang, Y. Liu, F. Ning, and Z. Feng, "Performance analysis of joint radar and communication enabled vehicular ad hoc network," *2019 IEEE/CIC International Conference on Communications in China, ICCC 2019*, no. Iccc, pp. 887–892, 2019.

[11] D. Ghozlani, A. Omri, S. Bouallegue, H. Chamkhia, and R. Bouallegue, "Stochastic Geometry-based Analysis of Joint Radar and Communication-Enabled Cooperative Detection Systems," pp. 325–330, 2021.

[12] J. P. Jeyaraj and M. Haenggi, "Cox models for vehicular networks: Sir performance and equivalence," *IEEE Transactions on Wireless Communications*, vol. 20, no. 1, pp. 171–185, 2021.

[13] Y. Sun, Z. Ding, X. Dai, K. Navaie, and D. K. C. So, "Performance of downlink noma in vehicular communication networks: An analysis based on poisson line cox point process," *IEEE Transactions on Vehicular Technology*, vol. 69, no. 11, pp. 14001–14006, 2020.

[14] C.-S. Choi and F. Baccelli, "Los coverage area in vehicular networks with cox-distributed roadside units and relays," *IEEE Transactions on Vehicular Technology*, pp. 1–11, 2023.

[15] G. Nigam, P. Minero, and M. Haenggi, "Coordinated multipoint joint transmission in heterogeneous networks," *IEEE Transactions on Communications*, vol. 62, no. 11, pp. 4134–4146, 2014.

[16] F. Baccelli and A. Giovanidis, "A stochastic geometry framework for analyzing pairwise-cooperative cellular networks," *IEEE Transactions on Wireless Communications*, vol. 14, no. 2, pp. 794–808, 2015.

[17] C. Skouroumounis, C. Psomas, and I. Krikidis, "Fd-jcas techniques for mmwave hetnets: Ginibre point process modeling and analysis," *IEEE Transactions on Mobile Computing*, vol. 21, no. 12, pp. 4352–4366, 2022.

[18] F. Mani, *Improved Ray-Tracing for advanced radio propagation channel modeling*. PhD thesis, UCLouvain, 2012.

[19] J.-E. Berg, "A recursive method for street microcell path loss calculations," in *Proceedings of 6th International Symposium on Personal, Indoor and Mobile Radio Communications*, vol. 1, pp. 140–143 vol.1, 1995.